Molecular characterization of polyimide film and silicone adhesive outgassing using mass spectrometry

Jean-François Roussel, David Lansade, Ludivine Leclercq, Carlos Soares, John Alred, Martin Maxwell, Anthony Wong, John Anderson, Delphine Faye, Guillaume Rioland

Molecular Characterization of Outgassing of Polyimide Film and Silicone Adhesive Utilizing ASTM-E-1559 Mass Spectrometry

Jean-François Roussel,[1] David Lansade,[2] Ludivine Leclerc[3]
ONERA-DPHY, Université de Toulouse F-31055 Toulouse, France

Carlos E. Soares,[4] John M. Alred,[5] Maxwell G. Martin,[6] Anthony T. Wong,[7] John R. Anderson[8]
Jet Propulsion Laboratory, California Institute of Technology, Pasadena, CA, 91107, USA

and
Delphine Faye,[9] Guillaume Rioland[10]
CNES - French Aerospace Agency, 18 Avenue Edouard Belin, F-31401, Toulouse, Cedex 9, France

Prediction of contaminant levels is paramount to controlling and reducing their impact on space missions. In the recent years, it has become clear that a real breakthrough could only be achieved through a change of paradigm, namely by going beyond the classical characterization of total contaminant mass and rather characterizing the various emitted chemical species individually, both quantitatively and chemically. This article first reviews the methodology proposed to achieve this objective and then its implementation on two examples of materials (Black Kapton® and NuSil CV4-2946), on the basis of existing ASTM-E-1559 outgassing data including mass spectrometry data (MS). We show that the thermogravimetric analysis performed on the contaminant deposits (heating at 1 K/min) allows a good enough time-separation of chemical species to analyze and often identify them through their mass spectra. In turn, the knowledge of the fragments constituting their spectra allows an improved analysis of the MS data collected during the initial outgassing phase. The outgassing time-profiles of each of these chemical species then tells a lot about their actual outgassing physical laws. On the two studied materials, outgassing physics were found to be consistent with Fickian or non-Fickian diffusion, rather than with residence time desorption. After confirming these findings with more specific and more sensitive experiments, the door will be open to greatly improve assessments of contaminant amounts and nature in flight, through realistic multispecies physical models.

[1]Research Engineer, DPHY Department of Physics Instrumentation Environment Space, Jean-Francois.Roussel@onera.fr
[2]Research Engineer, DPHY Department of Physics Instrumentation Environment Space
[3]Research Engineer, DPHY Department of Physics Instrumentation Environment Space
[4]Principal Engineer, Group Supervisor – Contamination Control Engineering; Propulsion Thermal and Materials Engineering Section
[5]Technologist, Contamination Control Engineering, Propulsion Thermal and Materials Engineering Section
[6]Systems Engineer; Contamination Control Engineering, Propulsion Thermal and Materials Engineering Section
[7]Technologist; Contamination Control Engineering, Propulsion Thermal and Materials Engineering Section
[8]Technologist; Contamination Control Engineering, Propulsion Thermal and Materials Engineering Section
[99]Contamination Engineer, Laboratories and Expertise Department
[10]Contamination Engineer, Laboratories and Expertise Department

I. Introduction

As spacecraft designs improve, scientific goals become more ambitious requiring more sensitive instruments. As instruments are designed for more sensitive scientific goals, they also become more sensitive to the contamination of the scientific data. This in turn has driven developments in the contamination control discipline. For example, to address the question of potential past life on Mars the Perseverance rover required strict control over elements of interest and any organic carbon of terrestrial origin which could potentially contaminate the samples now being taken on Mars. Outgassing is a primary contamination source which must be predicted and mitigated to allow for the detection of organic signatures on mars. In addition to Mars 2020 (the Perseverance rover), missions such as Mars Sample Return, Europa Clipper, Europa Lander and SPHEREx all are highly sensitive to outgassing contamination and require that outgassing be comprehensively understood. This necessitates developments of new experimental and modeling techniques to quantify outgassing contamination and predict its effect on scientific goals.

Technically, spacecraft contamination analysts still face many practical challenges. Extrapolating weeklong ground tests to mission timescale, assessing contaminant sticking and possible reemission, understanding and quantifying radiation synergies, etc. are some of them. In the recent years, it has become more and more obvious that a real breakthrough can only be achieved thanks to a molecular level characterization providing a per species physical modeling [1], [2].

Only a realistic physics and chemistry-based model can allow extrapolation to such —much longer— timescales, or to different temperature conditions as experienced by space missions. Additionally, only a per species chemical characterization of contamination processes, whether outgassing, deposition, reemission or environmental synergies, can lead to the unravelling of physical laws. It can be verified easily that total mass measurements, as done on quartz crystal microbalances (QCM), can be modeled as a sum of almost any physical law, provided they involve enough free parameters and mathematical “pseudo-species”. This is the weak point of the European approach pursued since the 1980s [3], even though it has the advantage of being multi-species and allowing for fitting multi-temperature-step data. Nothing guarantees that the mathematical “pseudo-species” in such models correspond to real chemical species. If per species experimental characterization is made available, numerical simulation approaches would be different, since constraints on each species’ behavior versus time and temperature would have stronger physical correlation, probably only matching the right physical model.

Implementing this molecular species characterization, or species separation, yet remains a challenging and demanding program. Experimentally, it should rely on *in situ* species-level characterization technique, such as mass spectrometry. The superposition of all the fragments generated from all chemical species in the ionization chamber of a mass spectrometer (MS) often make this task difficult or intractable. Some physics-based separation technique ahead of the MS is thus needed, as in gas chromatography - mass spectrometry (GC-MS). However efficient as GC-MS species separation is, it cannot be implemented *in situ* and in real time. In this context, coupling of thermogravimetric analysis (TGA) with MS, even though it only implements a partial species separation, seems more promising and has been successfully used[2], [4]–[6]. Numerical processing of these rich MS data is just as challenging. In the general case, most of the measured mass signals (a given mass over charge ratio) still result

from fragments coming from the few molecules being reemitted at a given time, since species separation by TGA is only partial (reemission peaks somewhat overlap, or can sometimes be a real mixture of several species).

In parallel to this ambitious experimental and numerical program, we examined a simpler set of experimental data that is both readily available and suitable for simpler numerical analysis. Some of the considered ASTM-E-1559 [7] test data precisely turned out to contain good enough mass-spectrometry data while staying simple enough, with few outgassed species, to be processed "manually". Data and analysis presented here are those of Black Kapton® outgassed at 105 °C and NuSil CV4-2946 at 45 °C. We considered them worth publishing in this standalone article since they constitute both a valuable example proving species separation is feasible on the basis of TGA/MS data, even with simple processing in simple cases, and also actual data for these commonly used materials.

The organization of this article follows the logics of the species separation analysis, which we also want to demonstrate in these reasonably simple cases. So, in a non-chronological order, we first report the thermogravimetric analysis (TGA) of the deposits, using both the global reemission data from a quartz crystal microbalance (QCM) and the subsequent flux measured by the mass spectrometer. The important point demonstrated there is that the TGA implements a good enough species separation to determine the MS spectra of the reemitted chemical species. This is done successively for NuSil CV4-2946 (a thermally conductive silicone resin) and Black Kapton® (an opaque polyimide film).

Based on the knowledge of these MS spectra as measured in these conditions, a second section deals with outgassing data measured by the mass spectrometer (chronologically the first step, of course). There, all outgassed species are detected simultaneously, making their separation more complex in general. However, the knowledge of each outgassed species spectrum, and their small number in this case, allow separating them and determining their outgassing behavior. These results are then analyzed in view of the possible physics at play.

Finally, conclusions and perspectives are discussed, in particular in relationship to the global objective of being able to perform a similar analysis in more complex cases, with more species emitted, or in non-isothermal cases.

II. Thermogravimetric Analysis

Nusil CV4-2946 and Black Kapton® materials were selected as candidates for this work as they are both commonly used materials for aerospace applications and had already been tested for a recent JPL mission, so the data was readily available. Both materials were tested under ASTM-E-1559 Method B (cf. setup on Figure 1), which was then modified to incorporate two periods of Thermogravimetric Analysis, one for a beginning portion of the test, and the other for the remainder of the test. The first TGAs of the two materials were performed after 24 hours outgassing, following ASTM-E-1559 recommendations. The constant outgassing temperatures of these tests were 45 °C and 105 °C respectively. The test temperatures were originally selected to match the temperatures those materials would experience during the mission they were tested for. Because the principle of this study was using preexisting data, the temperatures were constrained by those previous test parameters.

TGAs were performed from 80 to 348 K at 1 K/min on the QCM on which the outgassed contaminants were deposited. Other TGAs were performed after the next deposition phases, which lasted a couple of days each, but

the smaller amount of deposited matter did not provide more interesting results, and these other TGAs are not presented here.

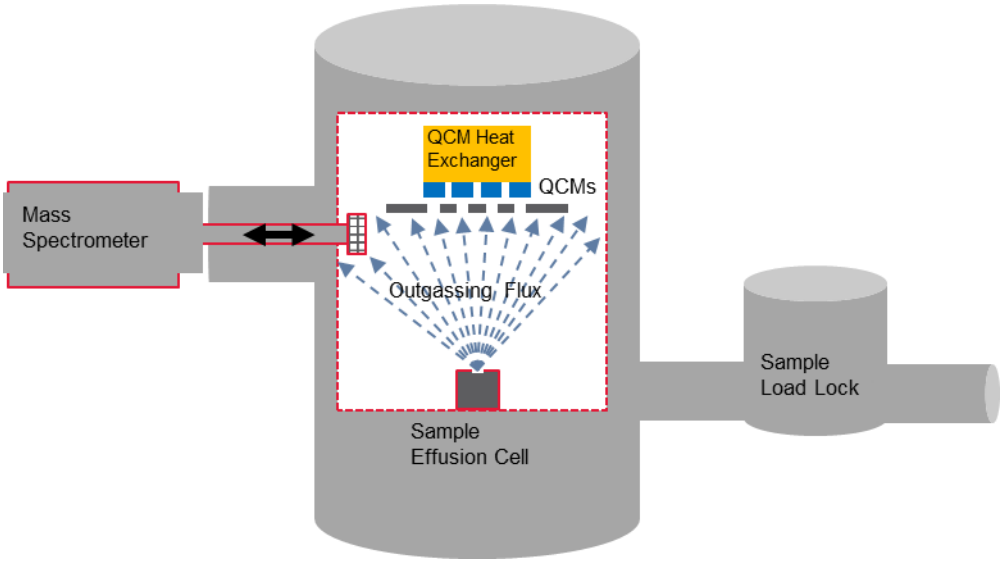

Figure 1: Illustration of ASTM-E-1559 Testing Chamber

A. NuSil CV4-2946

The CV-2946 samples were prepared using the prescribed 20:1 ratio of Part A:B. The samples also contain 0.5% pbw of solid glass microspheres. The samples were prepared on January 16, 2020, and were allowed to cure at room temperature until the start of this outgassing test (77 days). Four of the supplied adhesive discs were placed in the effusion cell on-edge as the test sample. The discs were placed in an aluminum foil pan on a metal clip so as to allow full exposure of all surfaces. The aluminum pan and the metal clip had been precleaned by methylene chloride rinse and vacuum baking. Disc dimensions and their initial masses were measured prior to the start of the outgassing test and were all close to (up to 5% individual variability maximum): diameter 1.27 cm, thickness 0.66 cm, mass 1.05 g (total mass 4.24 g).

The evaporation rate of contaminants as a function of the QCM temperature is plotted on Figure 2 upper panel. Two main peaks are visible: one in the 130-160 K region and a second one around 170 K. Other smaller overlapping peaks can be seen between 190 and 230 K. Finally, barely distinguishable peaks are found between 320 and 340 K, which will not be interpreted as no detectable reemission signal above the measurement noise level were found in MS data.

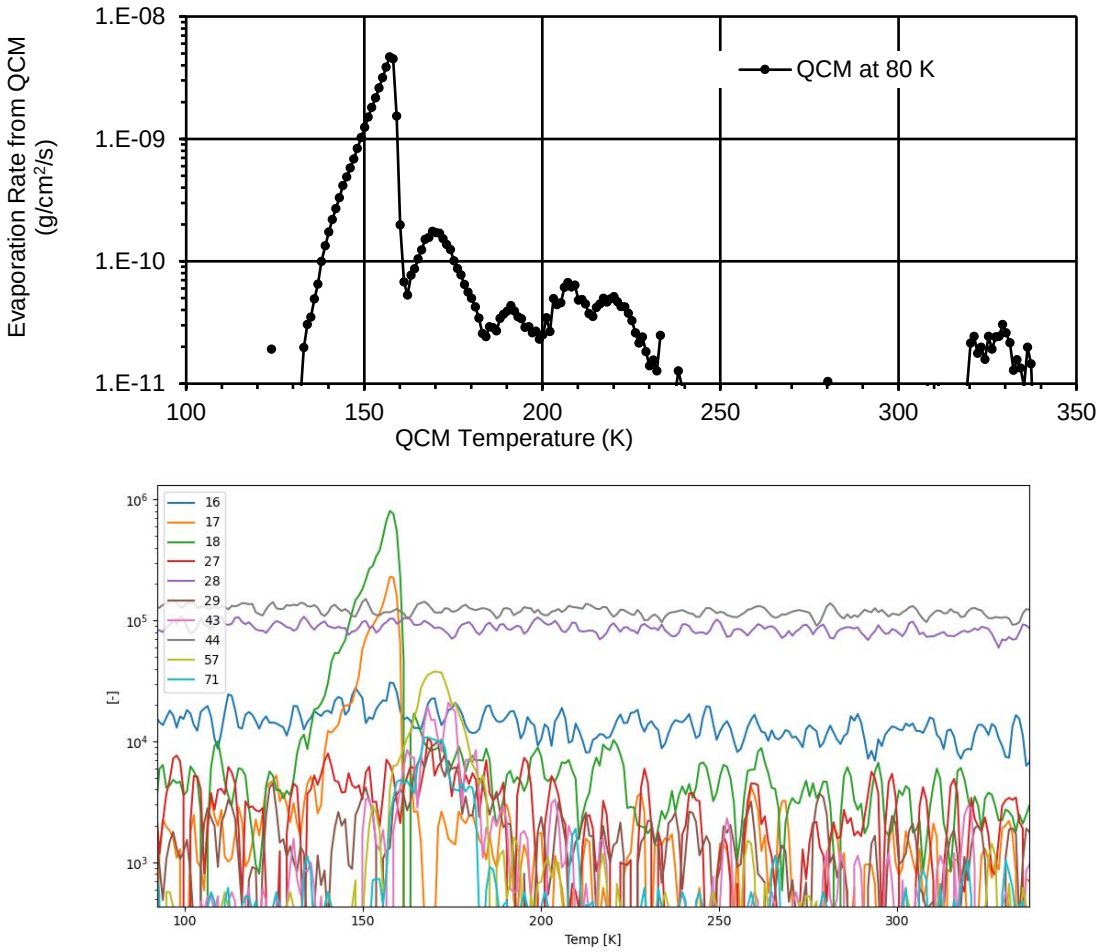

Figure 2: Thermogravimetric analysis of NuSil CV4-2946 Adhesive after 24 hour outgassing at 45°C: Evaporation rate from a QCM (upper panel) and mass spectrometer signals of selected masses (lower panel, arbitrary units) as a function of QCM temperature (common x-axis).

In order to determine which molecules are being reemitted during the TGA, mass spectrometry data were acquired concomitantly. Selected data are presented on Figure 2 lower panel where the signal intensities are represented as a function of temperature. Some mass channels are representative of the chamber background, m/z = 44 for CO_2, 32 for O_2 or 16 for the O fragment. Others are here to represent the baseline of the mass spectrometer, i.e. their signals do not increase at any time during the TGA. Some masses, namely m/z = 17, 18, and 57 clearly present observable peaks with maximum intensity at 158 K (m/z = 17 and 18) and 170 K (m/z = 57). Masses 17 and 18 were clearly identified as ions originating from water and being the sole contributor to the peak observed in TGA between 130 and 160 K. Though this point is not further explored in this paper, it is thought that the small shoulder observed around 136K might be due to the glass transition of ice on the QCM [8].

Another way to visualize mass spectrometry data is to compile spectra on the whole range of the mass spectrometer (Figure 3), at given temperatures of interest (temperature at which peaks are observed on the QCM during the TGA). There are plotted histograms recorded by the mass spectrometer during TGA in the range 0 to 600 a.m.u. at 130, 150, 170, 210 and 220 K. A focus on the 0 to 120 a.m.u. region is presented in Figure 4. What was clear

on Figure 2 is confirmed: at 150 K, the sole contributors to mass spectrometer signal are masses 17 and 18, reiterating the idea that water is the contaminant reemitted at this temperature.

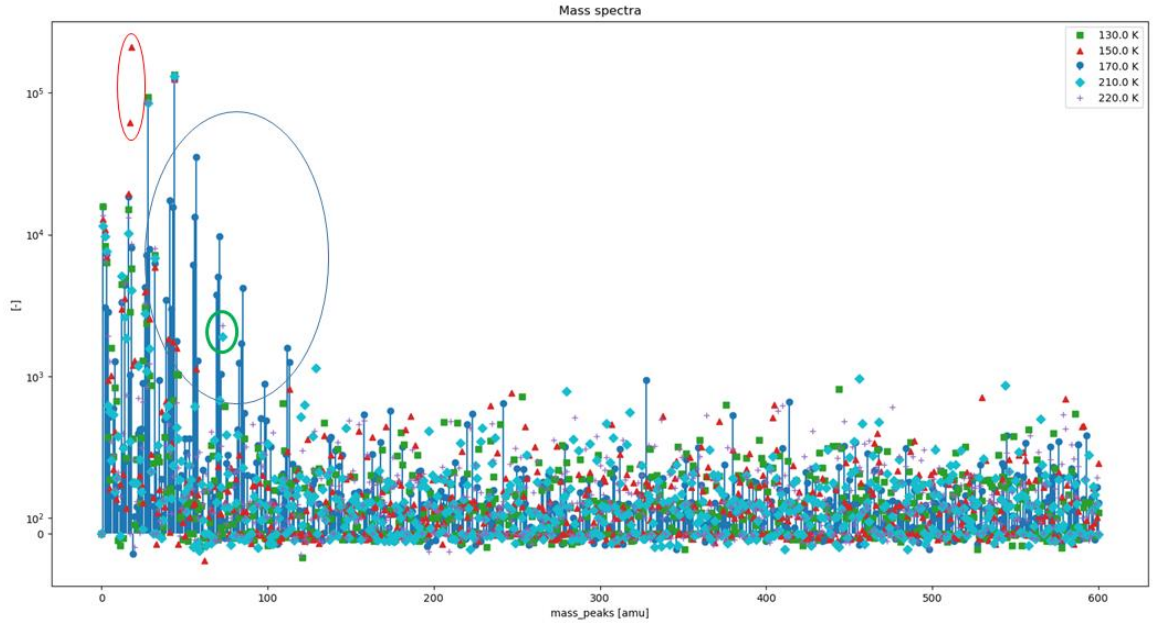

Figure 3: Superimposed mass spectrometry histograms of reemitted contaminants at 130 K (background), 150 K (water peak, cf. red circle), 170 K (main peak after water, cf. blue circle), 210 K and 220 K (minor peak, cf. green circle) over the whole range of the spectrometer (0 to 600 a.m.u.).

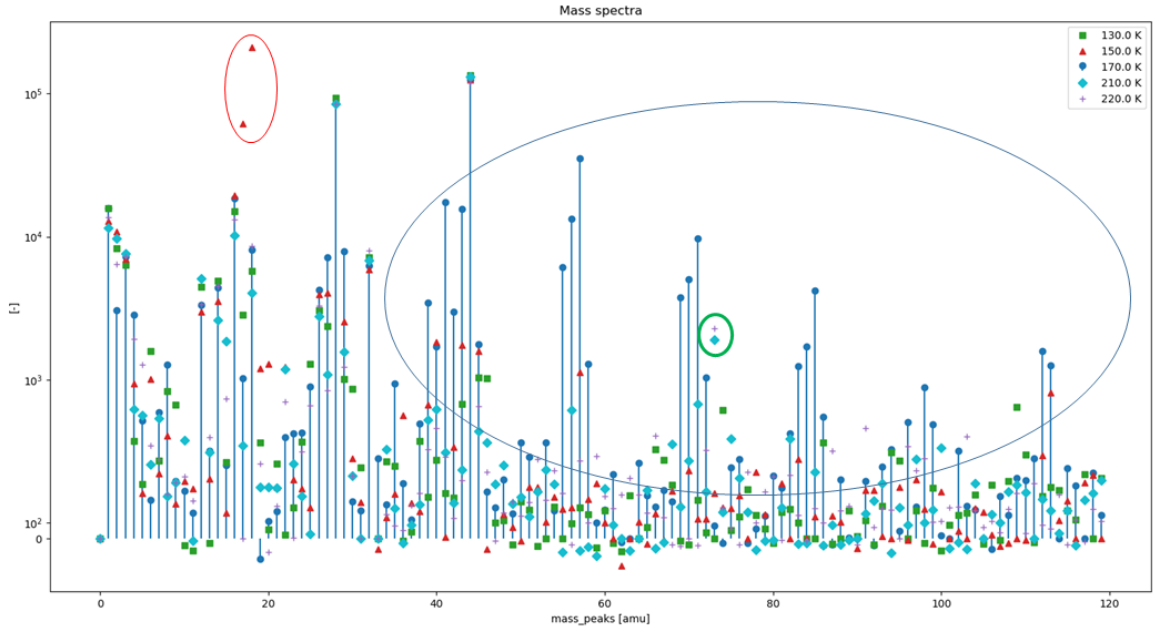

Figure 4: Superimposed mass spectrometry histograms of reemitted contaminants at 130 K (background), 150 K (water peak, cf. red circle), 170 K (main peak after water, cf. blue circle), 210 K and 220 K (minor peak, cf. green circle) in the 0 to 120 a.m.u. region.

At 170 K is observed a signal pattern with peaks separated by a pseudo-period of 14 a.m.u., characteristic of the presence of alkyl fragments. The heaviest mass peak seems to be 114 a.m.u., suggesting the presence of an alkane such as octane (C_8H_{18}), possibly mixed with shorter alkanes as well. Figure 5 represents the mass spectrum of octane as found in the NIST mass spectra database [9]. The resemblance with our data is striking especially regarding the known pattern where a "signal gap" between the 114 a.m.u. fragment and the previous at 85 a.m.u. is observed.

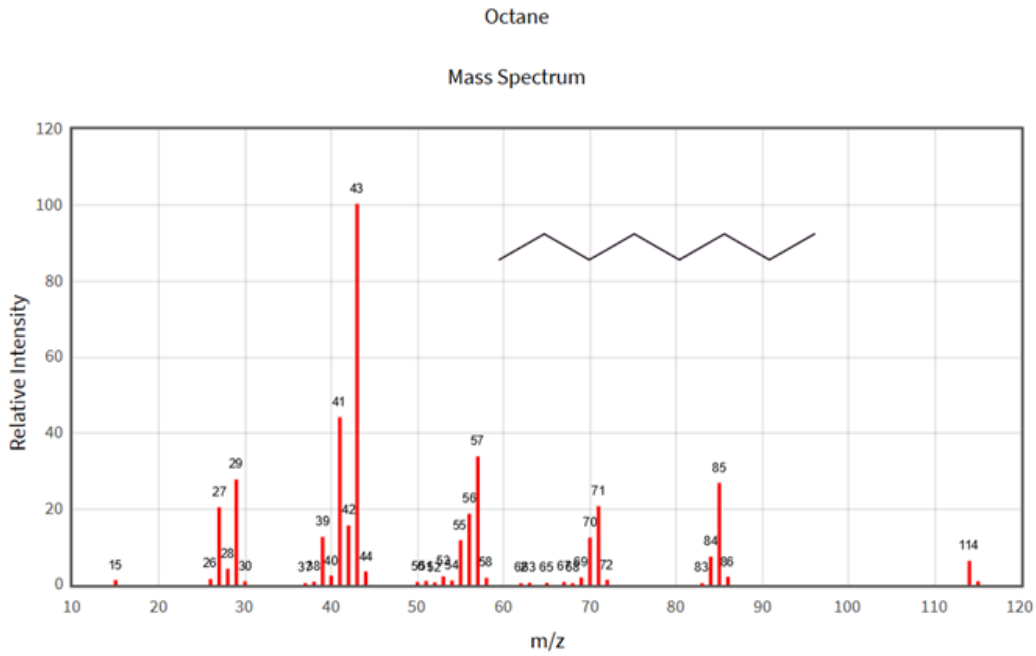

Figure 5: Mass spectrum of octane extracted from the NIST database [9]

In order to validate the hypothesis of octane being the molecule responsible for the TGA peak at 170 K, the octane fragments shown on Figure 5 were plotted together as a function of temperature in Figure 6. A well-defined peak is observed, with all signals having proportional intensities (parallel curves in log scale). This is consistent with the idea that all these signals originate from the same molecule, namely octane. Only mass 29 has a larger baseline, probably due to background $^{15}N^{14}N$.

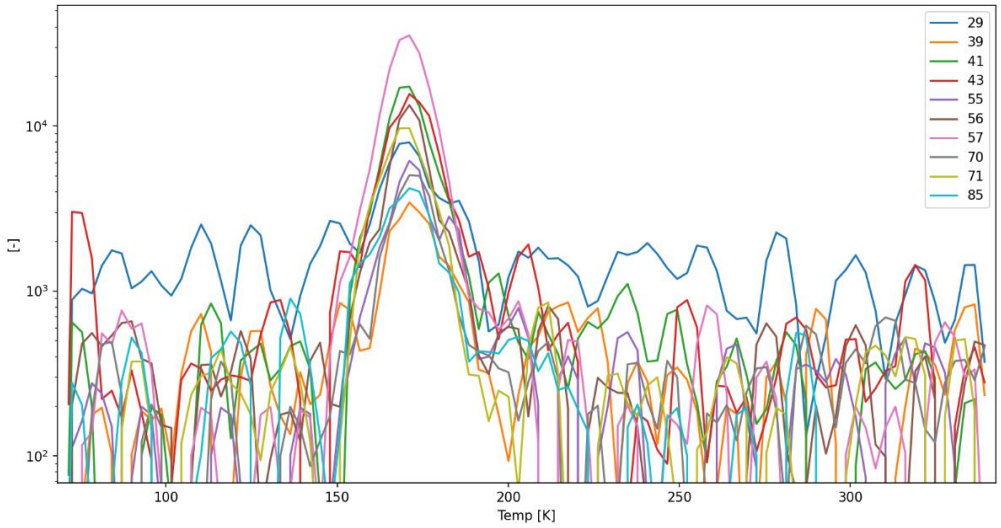

Figure 6: Mass spectrometry signals of fragments known to originate from octane. The peak at 170 K becomes obvious.

At higher temperature, things become less clear, though it is possible to observe in Figure 7 a faint signal for mass 73 a.m.u. in the 200-230 K range, which could be responsible for TGA peaks around 210 and 220 K. Despite the fact that there is not much signal in the mass spectrometer to corroborate this idea, a possible candidate for this fragment would the trimethylsilyl radical ($Si(CH_3)_3$). Concerning observable TGA peaks at 320-340 K, no mass spectrometry data were significant enough to try and identify any contaminant.

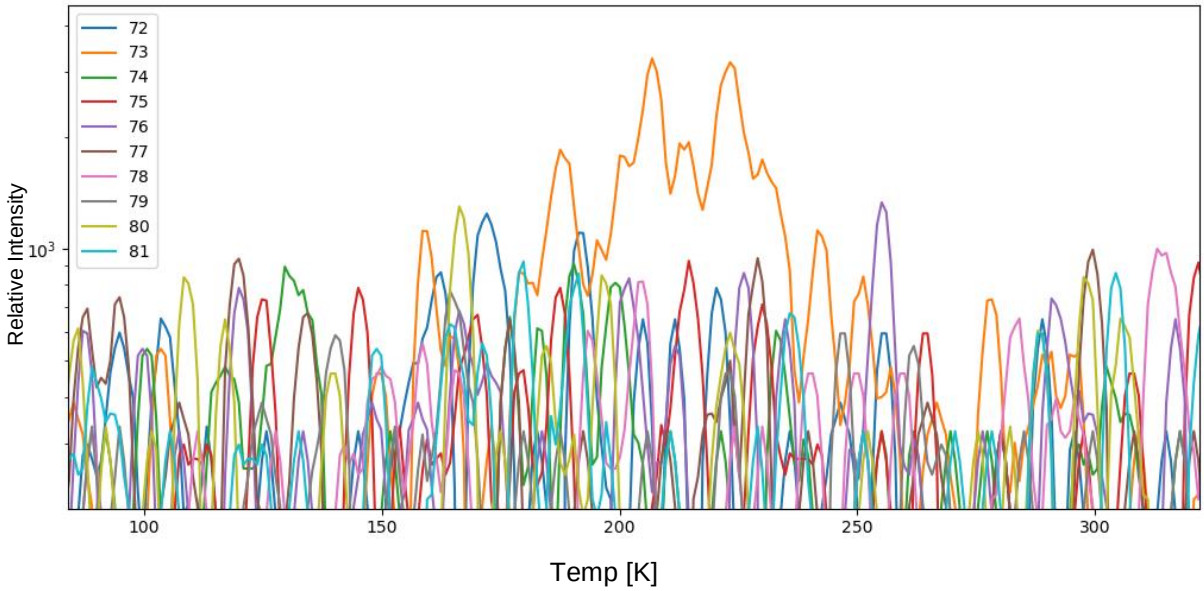

Figure 7: MS signals of mass 73 and masses around representative of noise. A faint signal is visible for mass 73 around 205- 225 K, a factor around 3 above the noise. No other mass channels were found to exhibit a signal around that temperature.

In this part, it was shown that at least two different molecules and a fragment were identified as contaminants reemitted during TGA, namely water, octane and probably trimethylsilyl respectively at 130-160, 170 and 210-220 K. The following part is dedicated to TGA experiments carried out on Black Kapton®.

B. Black Kapton®

The Black Kapton® sample used was a single sheet of material measuring 30.48 cm by 30.48 cm by 0.00254 cm thick. The entire supplied sheet of material was folded with 3.81 cm wide pleats and secured with a precleaned metal clip. This folded sheet was placed in the effusion cell on-edge as the test sample. The total surface area of the sample was 929.0 cm2 and the total mass of the sample was 3.456 g. The surface area listed above includes one face of the sheet and no edge area.

The evaporation rate of contaminants as a function of the QCM temperature is plotted on Figure 8 upper panel. Three peaks are neatly observed: one with a maximum at 165 K, one at 190 K and finally a third one at around 280 K, data above 300 K being only considered as noise again.

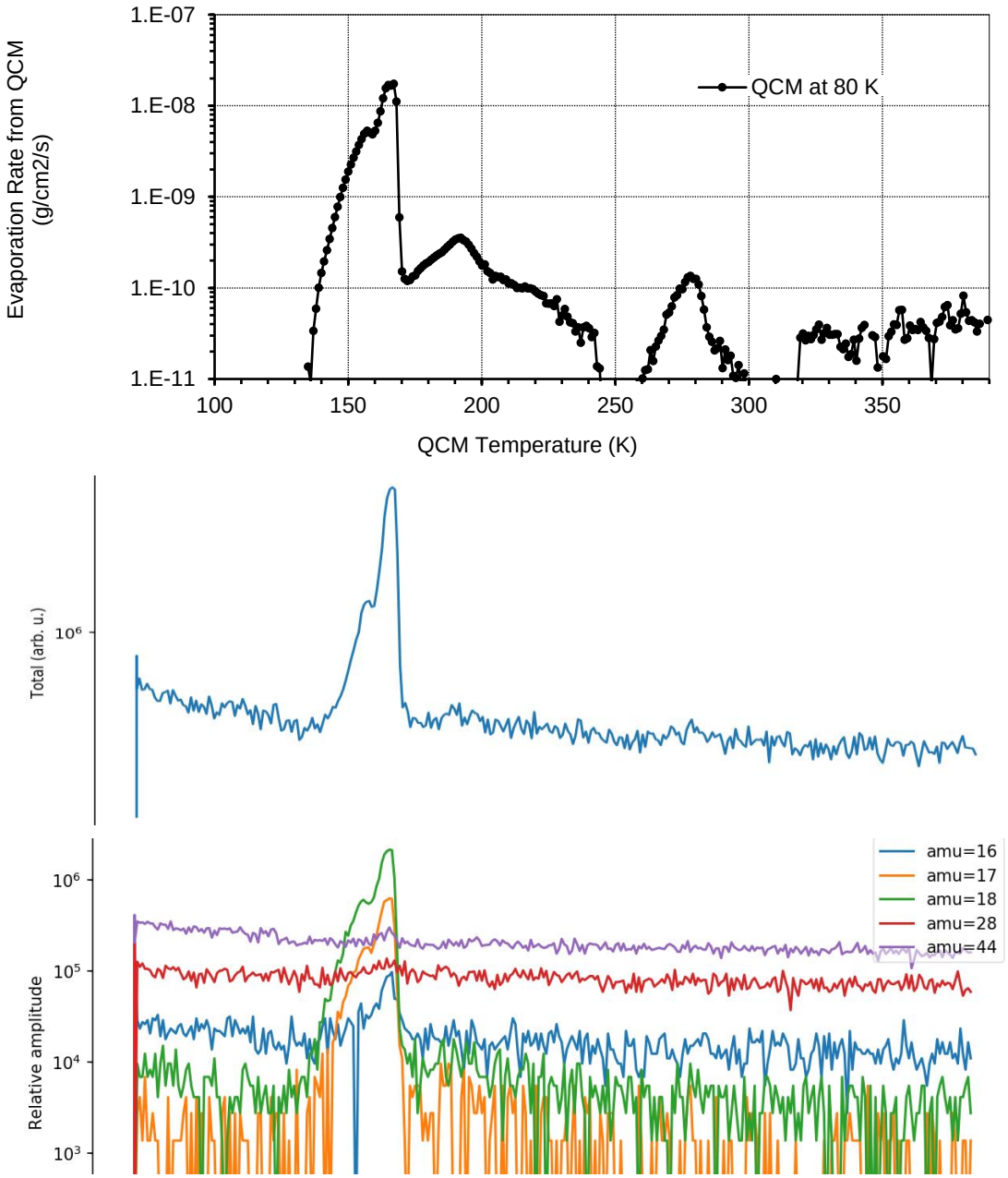

Figure 8: Thermogravimetric analysis of Black Kapton® deposit following 24 hours outgassing at 105°C: Evaporation rate from a QCM (upper panel), sum of all MS signals (middle panel), and MS signals of fragments known to originate from water and masses 28 and 44 a.m.u. to illustrate quasi steady masses (lower panel) as a function of QCM temperature (common x-axis).

Once again, mass spectrometry data were used to evaluate which contaminants were reemitted during the TGA. On Figure 8 middle panel is plotted the sum of all MS signals as a function of time. Peak number one at 165 K is conspicuous while the other detected ones during the TGA are barely visible. Plotting of masses 16, 17 and 18 a.m.u. as a function of time (Figure 8 lower panel) makes it clear that the first peak observed in TGA can be attributed to water as their signal all stick out at the same time in a coordinated fashion.

As previously mentioned, other signals than water in the mass spectrometry data are tough to find as it stands. Nevertheless, one way to discern extra signals would be to increase signal over noise ratio artificially. This is what

was done in Figure 9 where 15 spectra were averaged around a temperature of 190 K and compared to background (on the [183-196] K temperature range).

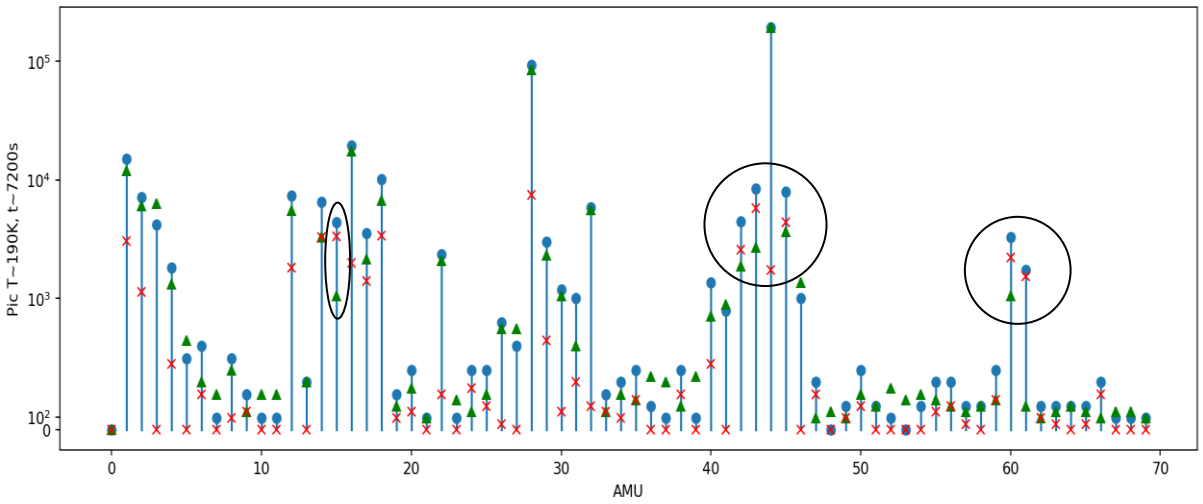

Figure 9: Averaged MS histogram around 190 K (blue circles) compared to background (green triangles), and difference 190K_signal – background (red crosses). Relevant masses are circled in black (large signal (blue circles) and differences (red crosses)).

New masses stand out: 61, 60, 45, 43, 42 and 15 a.m.u. Their signal intensities as a function of temperature are plotted in Figure 10. Though the presence of peaks is not as obvious as for water, one can see a meaningful rise in their signals somewhere between 175 and 220K, which corresponds to the quite broad second peak of QCM TGA. Mass 45 has a higher baseline, probably due to CO_2 molecules involving heavier C or O isotopes. As mass 61 seems to be the heaviest ion, it could be the molecular ion of the parent contaminant molecule. From MS databases a possible candidate with a quite similar spectral signature could be N,N-dimethylhydroxylamine (Figure 11) [10]. Two (or more) molecules might yet be involved as indicated by the width of the QCM peak and the complexity of MS signals of Figure 10. It must be noted that molecules and spectra obtained from GC/MS analyses of the exact material under scrutiny are another source of a smaller set of candidate molecules to be compared with these measurements. Unfortunately, GC/MS data from the original material was not available in this case.

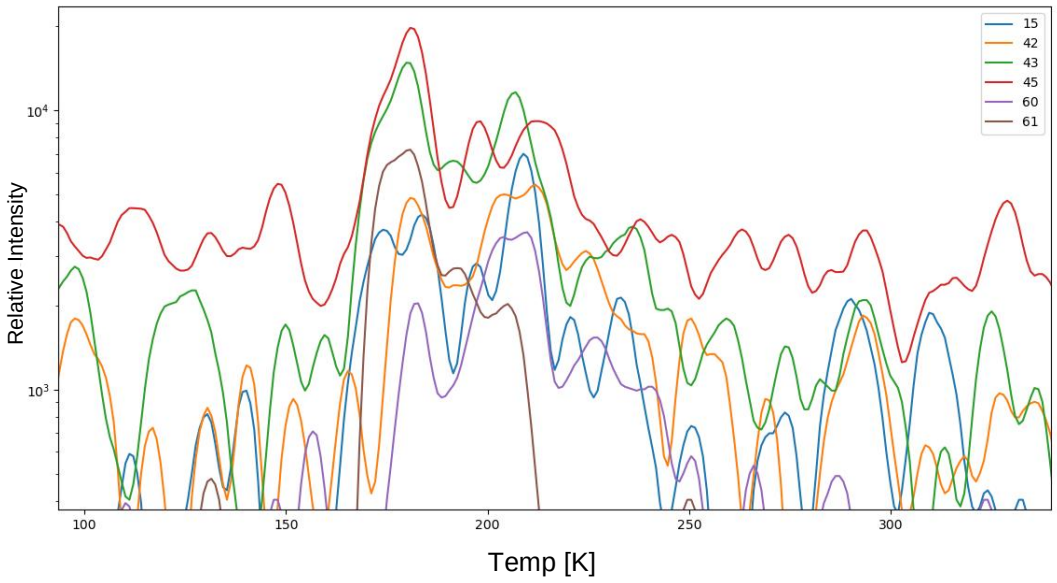

Figure 10: Mass spectrometry signals of selected fragments identified as being responsible for TGA peak around 190 K.

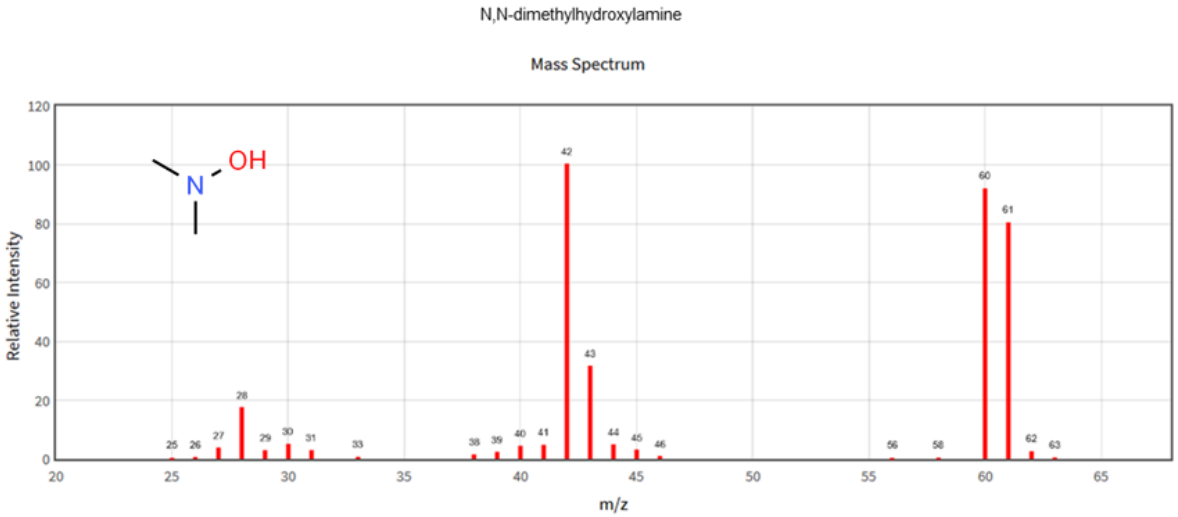

Figure 11: Mass spectrum of N,N-dimethylhydroxylamine extracted from the NIST database [10].

Concerning the third peak observed during the TGA at 280 K, only one mass shows up in the MS data with a m/z ratio of 58 a.m.u. (cf. Figure 12). If one considers this fragment to be the molecular ion, only a few molecules could fit with experimental data, mostly acetone or propanal (Figure 13). However no fragment with an m/z ratio of 43 a.m.u. sticks out in the data, which makes propanal a better candidate. Another molecule could as well be considered, azomethane $C_2N_2H_6$, but it should be discarded for the same reason as acetone.

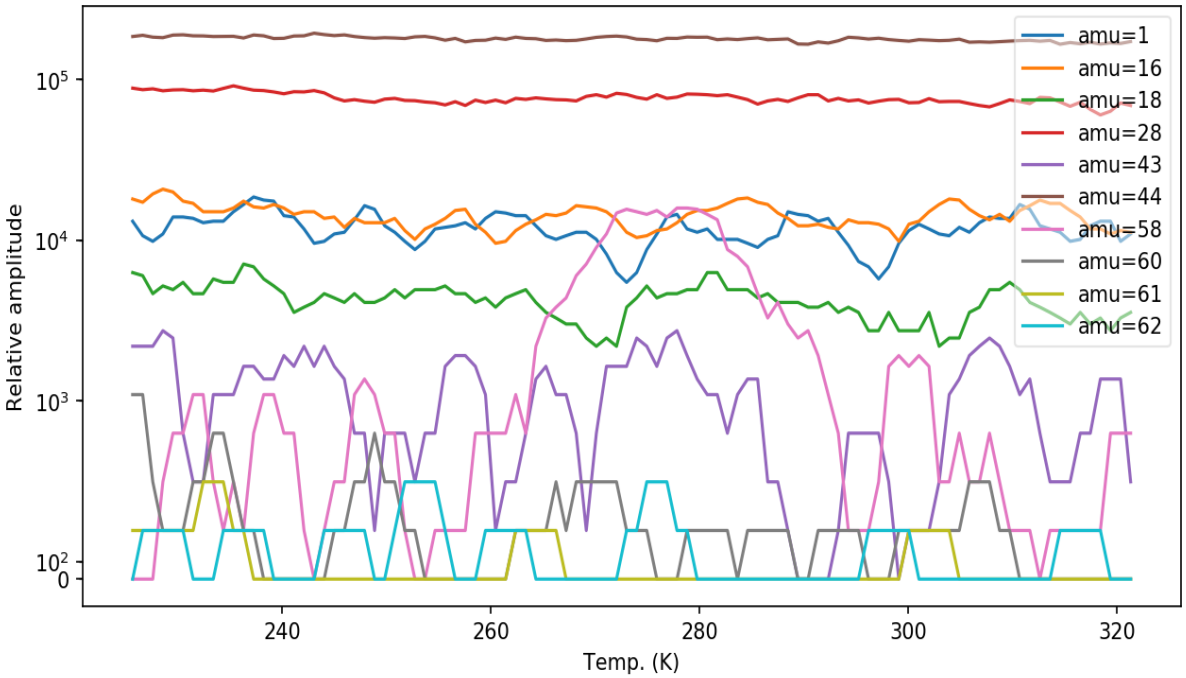

Figure 12: Mass spectrometry signals of selected fragments among which one stands out (58 a.m.u.) at 280 K.

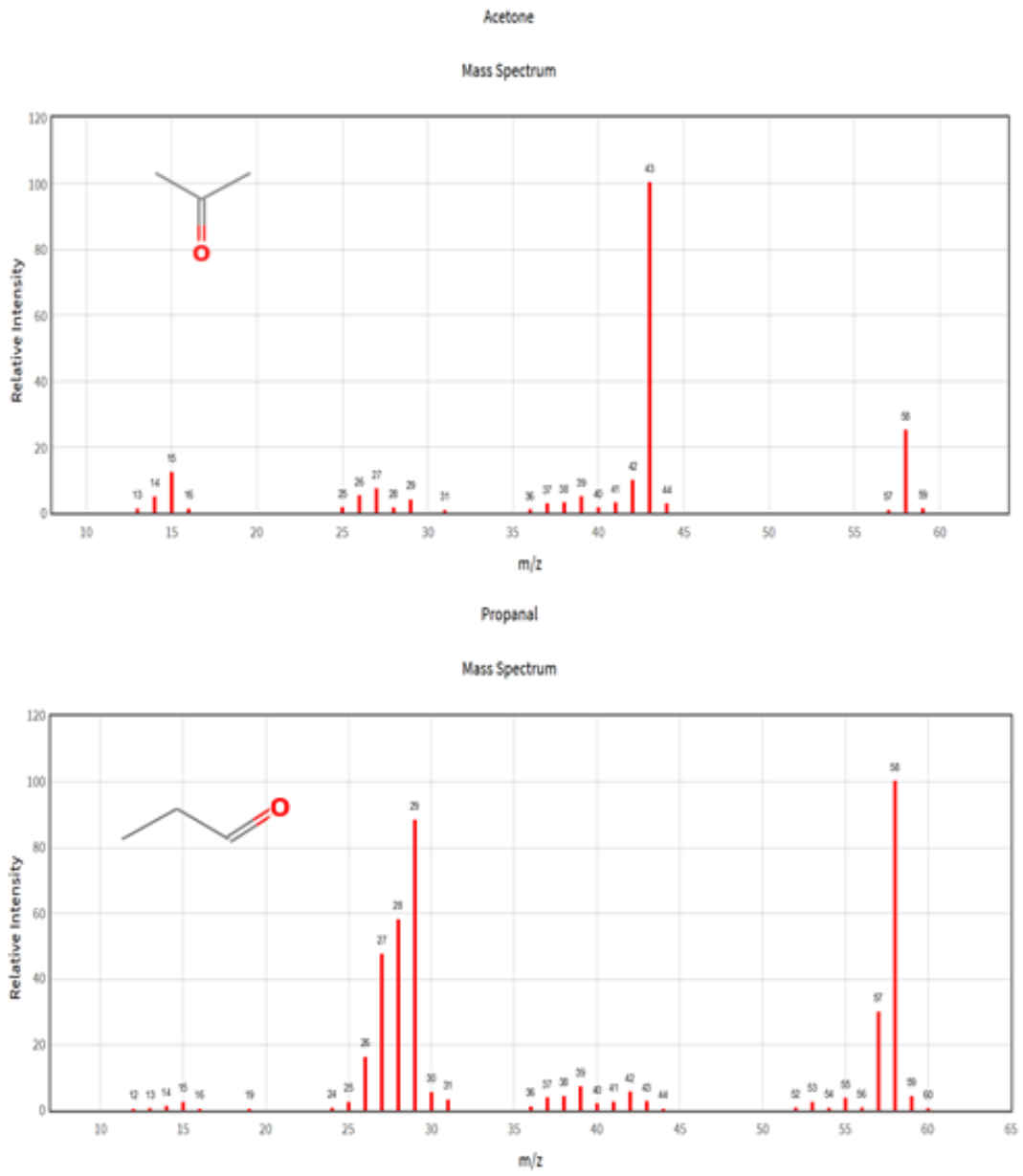

Figure 13: Mass spectra of acetone and propanal, possible candidates for molecules reemitted at 280 K, extracted from the NIST database [11], [12].

Clearly, the poor signal-to-noise ratio at this elevated temperature makes an unquestionable identification of the contaminant responsible for the peak at 280 K quite difficult. One way to increase the signal would be to outgas this material at higher temperature since all the phenomena responsible for outgassing (diffusion and desorption) are temperature-dependent. The mass of contaminants leaving the source material would be higher and so would be the mass deposited on the QCM. Alternatively, the more accurate GC-MS characterization is another way to reduce the list of candidate species for TGA-MS identification, but it was not performed for this material, since the logics of this study was to go as far as possible in species identification on the basis of "regular ASTM-E-1559" data

Nevertheless, three contaminants were identified as being reemitted during the TGA of Black Kapton®: water, N,N-dimethylhydroxylamine and possibly propanal, respectively at 160, 190 and 280 K.

III. Outgassing

Prior to the TGAs, materials were outgassed for 6 days at a constant temperature of 45˚C (CV4-2946) or 105°C (Black Kapton®), with measurements made both on QCM and MS (except for mass signals with m/z ratio lower than 29 during the first 24 h to avoid saturating the MS). After that first day, a TGA was performed, during which time, the Knudsen cell was removed from the chamber, and allowed to passively cool approaching ambient temperature, consequently reducing the sample's outgassing (done for Black Kapton® but not for Nusil). The materials were then heated up again to resume outgassing.

Now that species separation was performed thanks to TGA-MS data analysis, the knowledge of the species spectra should allow deducing their outgassing behavior. Mass spectra recorded during the outgassing are presented and analyzed in the following sections.

A. NuSil CV4-2946

During the TGA presented above, octane was thought to be the molecule responsible for the peak at 170 K. Masses representative of the ions coming from the fragmentation of light alkanes or octane are represented on Figure 14. Signals decrease in a parallel fashion, which on a semi-log plot demonstrates proportionality, consistently with the hypothesis of fragments originating from a same molecule. After decreasing for a while, these signals reach a minimum where they blend into the MS baseline.

Due to the way the digitalization of the measure is carried out in the MS, the signal is discretized into multiples of a base value of 1362. This means that along with time, a mass signal becoming smaller than 1362 will successively take values of 0 or 1362, likely with a probability more or less consistent with its distance to either value. As the data presented in this study are averaged over a few minutes, the original value may be approximately reconstructed even for values below 1362, but probably not correctly for values much below it (by one or several orders of magnitude).

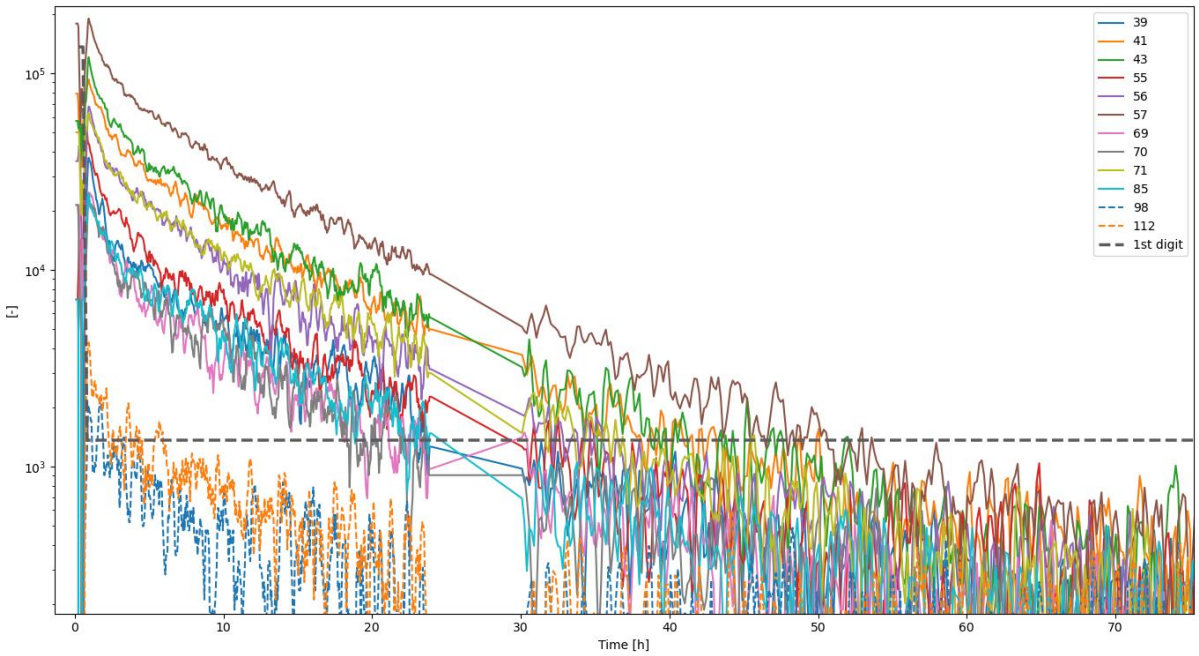

Figure 14: Mass spectrometry signals of fragments known to originate from octane during the outgassing step of NuSil CV4-2946.

Another way to look at this data is to plot multiple mass spectra measured at different times. Such a representation is given on Figure 15 where three mass spectra measured at 1, 10 and 100 hours are superimposed. They start at m/z ratio 29 since lower masses were not recorded during the first 24 h of the outgassing.

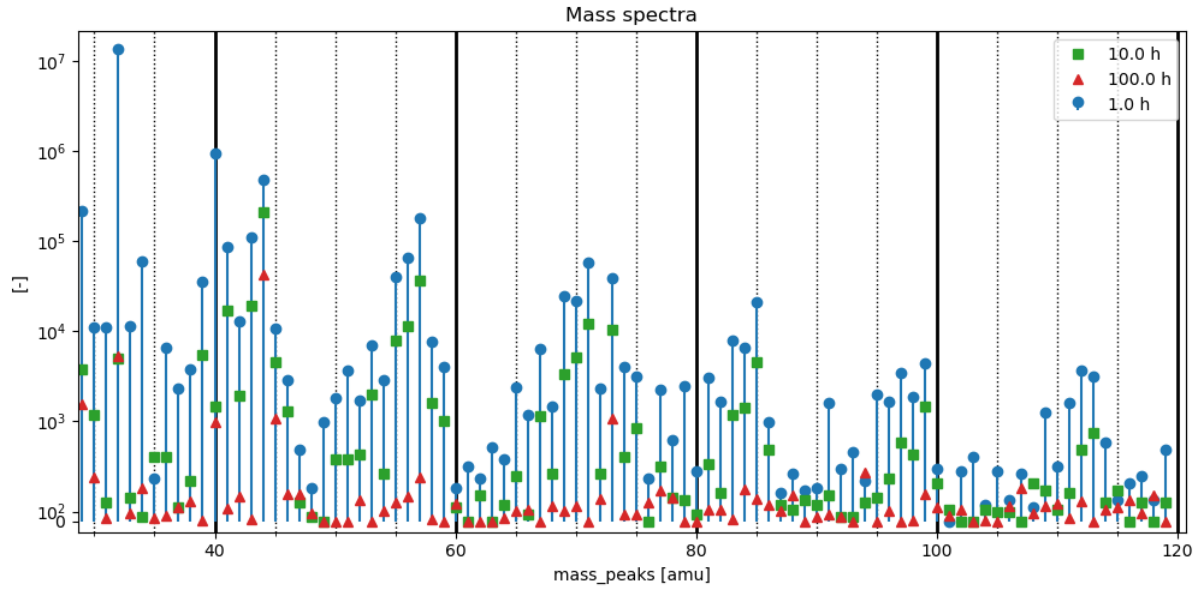

Figure 15: Superimposed mass spectrometry histograms recorded after 1, 10 and 100 h during the outgassing step of NuSil CV4-2946.

The two first stacked spectra (recorded respectively after 1 and 10 hours) show a net domination of the alkyls fragments in the composition of the outgassed species. This is consistent with what was seen during the TGA and previously described in part II-A) of this paper.

Now that at least one outgassed species was formally identified, it is of prime interest to find out which physics govern its outgassing behavior. In other terms, are the outgassing kinetics in phase with known diffusion laws in polymer materials?

In order to answer that question, MS signals of known alkyl fragments were plotted as a function of time in Figure 16. On top of these, three different laws were plotted to try matching these results on part or the entirety of the time series: one decreasing in $t^{-1/2}$, one in 1/t and finally one corresponding to the solution of a Fick law of diffusion (assuming that desorption at the material free surface is instantaneous, which results in a zero contaminant density at the surface).

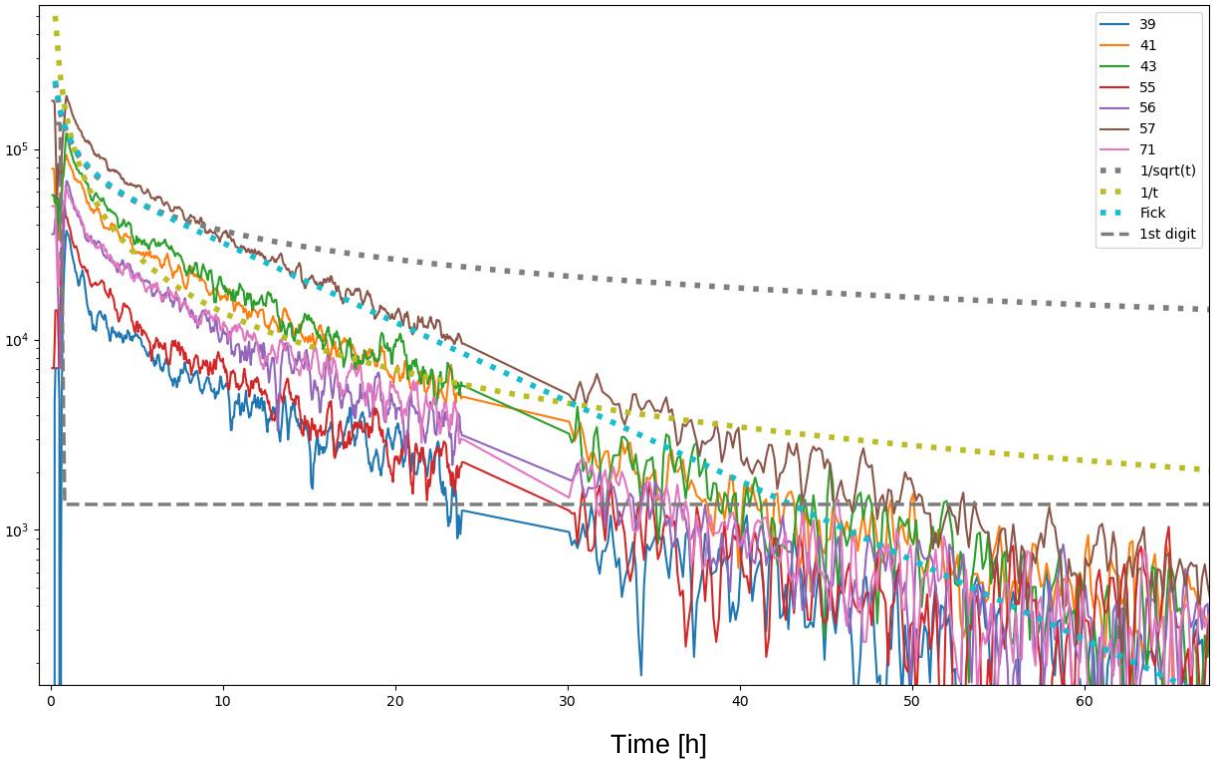

Figure 16: Mass spectrometry signals of alkyl fragments during the outgassing step of NuSil CV4-2946 and 3 different outgassing laws (one being Fickian with D=3,500 m^2s^{-1}, the two other ones decreasing in $t^{-1/2}$ and .1/t).

In this figure, one can see that the Fick's law of diffusion fits particularly well the experimental data, even though there is only one free parameter: the diffusion coefficient D that governs both the slope at long times (exponential asymptotic behavior) and the time of the transition between short times asymptotic behavior (decreasing in $t^{-1/2}$) and the long times one (in $e^{-t/\tau}$, showing linear on this semi-log plot). On the contrary the two power laws that were used to try fitting data here, only succeed so on a reduced time frame. By contrast the Fick law fit looks consistent

over the whole range of usable data, almost one decade lower than the "first digit" value (i.e. with values corresponding to the averaging of almost as little as one non zero value out of ten).

The same process was applied to mass 73, then attributed to a trimethylsilyl fragment, as can be seen in Figure 17, where alkyl and trimethylsilyl fragments as well as their corresponding Fick's law fits are superimposed. Both Fickian models fit their corresponding molecule quite well. The one fitting mass 73 implies the use of a diffusion coefficient 4 times smaller than the one for octane.

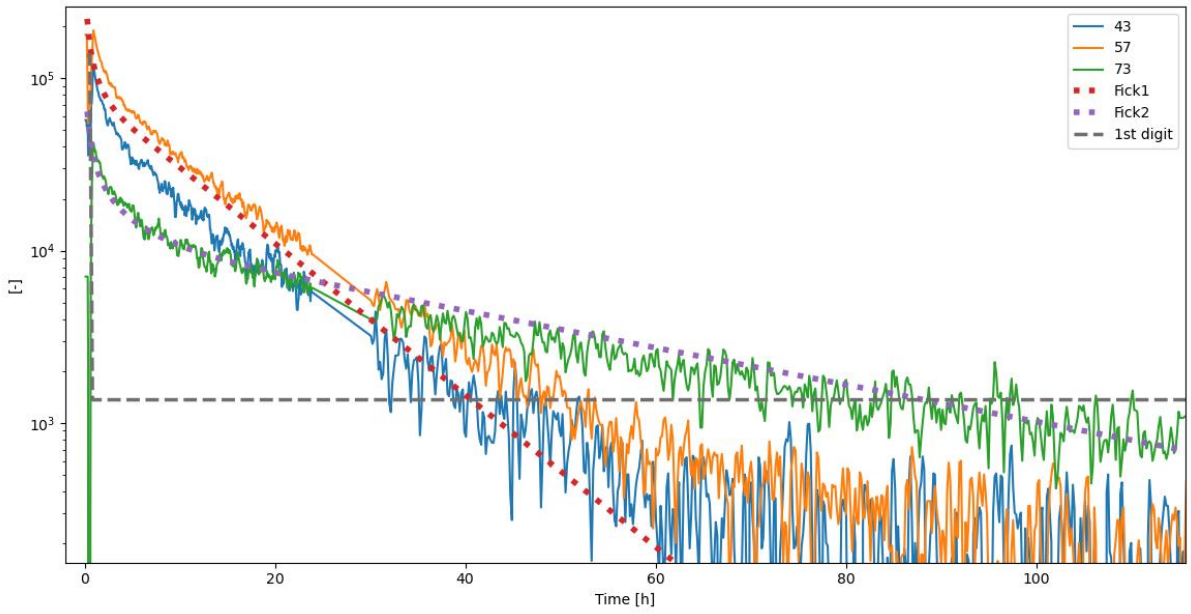

Figure 17: Mass spectrometry signals of main alkyl fragments and trimethylsilyl fragment during the outgassing step of NuSil CV4-2946 plotted against two solutions of Fick's laws with two different diffusion coefficients, D=3,700 m^2s^{-1} and 900 m^2s^{-1} respectively

To conclude with this part, it was shown that even with poor overall signal due to the low outgassing temperature (45 °C), three outgassed species from the NuSil CV4-2946 were identified, namely water and two other species probably being octane and $Si(CH_3)_3$. The last two were shown to be very consistent with Fickian laws of diffusion over two to three orders of magnitude.

In the following part of this discussion similar data processing concerning the outgassed molecules originating from Black Kapton® will be presented.

B. Black Kapton®

On Figure 18 are plotted the signal of several masses that were identified in part II as probably originating from N,N-dimethylhydroxylamine and propanal. Among these signals, 3 seem to have a very similar behavior (m/z 60, 43 and 42), *i.e.* they have similar relative intensities versus time, and one does not follow the same decreasing pace (m/z 58).

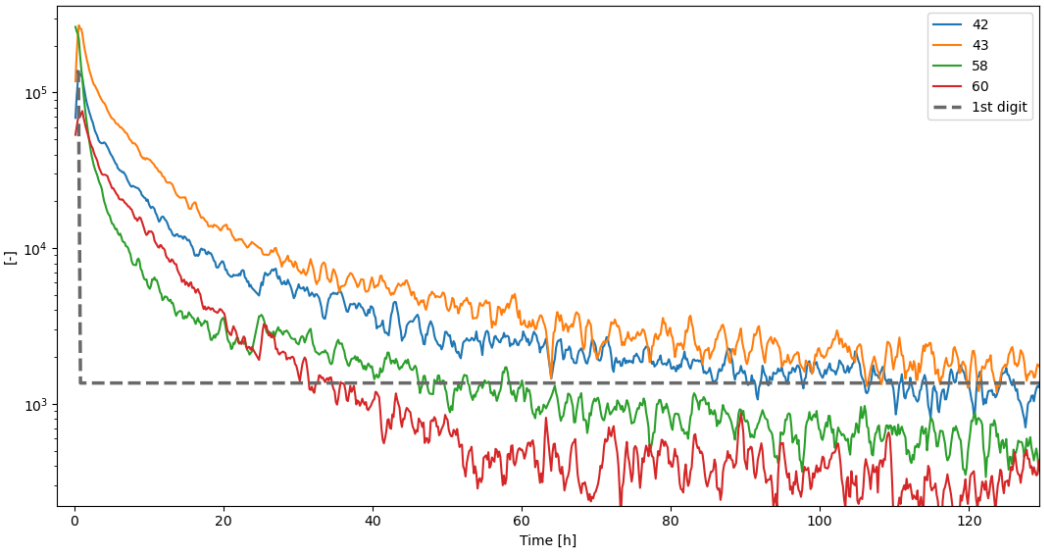

Figure 18: Mass spectrometry signals of fragments known to originate from N-N,dimethylhydroxylamine (42, 43, 60 a.m.u.) and propanal (58 a.m.u.) during the outgassing step of Black Kapton®

Attempts were made to fit these signals with Fick's law of diffusion as shown in Figure 19. On this figure, the same masses 60, 58, 43 and 42 are plotted versus time, with two different attempts of fitting them with a Fickian law.

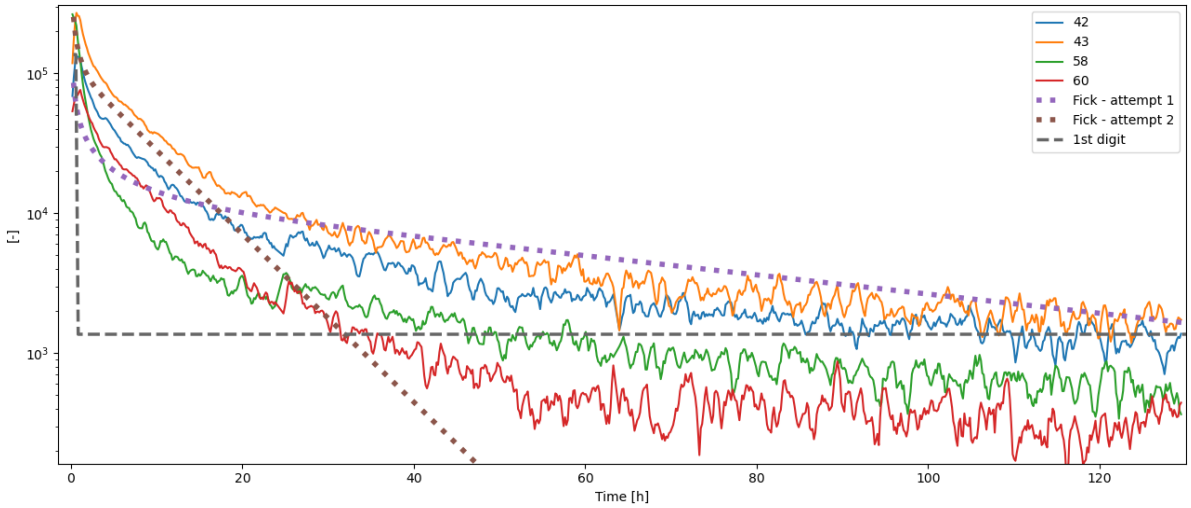

Figure 19: Mass spectrometry signals of main N-N,dimethylhydroxylamine and propanal during the outgassing step of Black Kapton® plotted against Fick's laws of diffusion.

Attempt 2 tries to fit the beginning of the data, i.e. roughly the first day of outgassing. Though this works well with early signal, this choice of parameters does not allow good fitting of the late data as it decays excessively fast afterward (data of the last days look significant as their values are larger than for NuSil adhesive in the previous case, and not much smaller than the first digitalization level). On the contrary, attempt 1 tries to fit the late data. Once again, though this works finely in the late region of the data, it appears that the transition between the initial asymptotic regime in $t^{-1/2}$ and the late one in $e^{-t/\tau}$ happens too early. It is to be noted that Fick's law of isothermal diffusion only has one free parameters to adjust: the diffusion coefficient D, or equivalently a time constant $\tau \sim$

L^2/D, which is roughly both the exponential decay time constant and the transition time between both regimes (and of course for this linear diffusion equation an overall multiplicative factor, proportional to the initial concentration).

Facing the impossibility to fit the data with Fick's law, other empirical power laws were tested as shown on Figure 20. A $t^{-1/2}$ model as well as a 1/t model were tested. The first one does not represent well the data as they decay much faster. On the contrary, the 1/t model seems to fit the data quite well, especially for the alkane fragments (mass 42, etc.), although it might not mean much more than a coincidence.

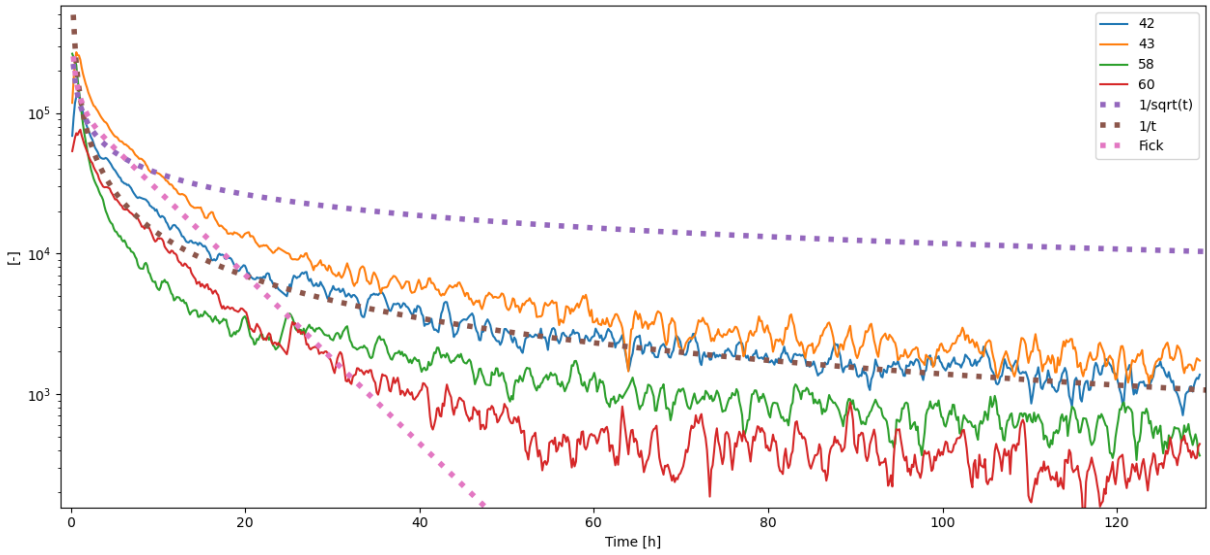

Figure 20: Mass spectrometry signals of main N-N,dimethylhydroxylamine and propanal during the outgassing step of Black Kapton® plotted against Fick's and power laws of diffusion.

Many factors could explain the difficulty for experimental data to be fitted with Fick's law of diffusion. Some possibilities are: the (un)swelling of the polymer network during outgassing, a change of the state of the three-dimensional network of the polymer matrix, coming close to the glass transition temperature (although here we are far below for Black Kapton®), or the fact that we might be also limited by desorption since the Fick's law solution under use assumes instantaneous desorption of molecules at the material free surface (zero-density boundary condition at the free surface).

IV. Conclusion

In this paper we presented the outgassing characterizations at molecular level from ASTM-E-1559 tests results of two space grade materials, namely NuSil CV4-2946 and Black Kapton®. These results were obtained by week-long isothermal outgassing of the materials, interrupted by several thermogravimetric analyses, in the presence of a mass spectrometer.

It was shown that this method allows the identification of outgassed molecules after they are reemitted from a heated QCM while performing a TGA. The recording of mass spectra allows the comparison with readily available spectra database and therefore identification of the reemitted molecules. It was demonstrated that for the materials shown here, at such low outgassing temperature, it was mainly water responsible for the mass loss of the materials.

Nevertheless, even with poor signal over noise ratio in the mass spectrometer, it was made possible to extract and tentatively identify up to two other contaminants per materials. In the case of NuSil CV4-2946 they are thought to be octane and trimethylsilyl though the latter is accompanied by a certain degree of uncertainty, whereas in the case of Black Kapton®, they are thought to be N,N-dimethylhydroxylamine and propanal, though the identification of the latter is as well stained with uncertainty.

With these results, it became possible to analyze outgassing data with the *a priori* knowledge of the outgassed molecules in such a way that one could try and figure out what the physical laws governing the outgassing are. In the case of NuSil CV4-2946 it was shown that besides water, the outgassing of the other two contaminants detected could be fitted satisfactorily with Fick's law of diffusion. On the contrary, in the case of Black Kapton®, neither N,N-dimethylhydroxylamine nor propanal could easily be fitted with a Fick's law, although some power law could work in some cases. At this point, it is not clearly understood why in the case of Black Kapton® this fitting does not work so well. Potential answers to this include more complex interaction between the contaminants and the polymer matrix, the swelling of the polymer matrix, the glass transition temperature of the polymer matrix or even a limitation of the outgassing process by desorption at the surface of the polymer matrix.

New experiments are currently being designed in order to improve the method presented in this paper. They include the possibility of outgassing materials at higher temperature, possibly with increasing temperature steps, in order to accelerate all the thermally activated processes leading to the deposition of contaminants on the cryogenic QCM. This would allow a higher surface concentration of contaminants on the QCM as well as a higher partial pressure of contaminants in the vicinity of the mass spectrometer, thus significantly raising the signal over noise ratio on both cases. Besides, in the results presented here, the identification of the reemitted molecules was done manually, which was only possible because of the small amount of molecules to be detected. In order to be able to treat data with a lot more information, the automation of the species separation must be achieved. This work is still in progress but should allow a much finer comprehension of the physics underlying the contamination processes and, *in fine*, authorize better prediction of the behavior of outgassing materials in space environment, based on chemistry and physical laws.

Acknowledgements

This research was carried out with the Jet Propulsion Laboratory, California Institute of Technology, under a contract with the National Aeronautics and Space Administration (80NM0018D0004). ONERA authors acknowledge CNES funding by contract number 4500063311/DIA094 and ONERA internal funding ref. RGF/CI/32129.

References

[1] Roussel J.-F., Faye D., Van Eesbeek M., Tondu T., Migliore R., Rampini R., and Paulmier T., "A new frontier for contamination: reaching the molecules," *Proceedings of the 11th ISMSE*, Aix-en-Provence, France, 2009, p. 11.

[2] Roussel J.-F., Tondu T., Paulmier T., Faye D., Van Eesbeek M., and Rampini R., "Progress on the Physical Approach to Molecular Contamination Modeling," *J Spacecr Rockets*, vol. 48, nº 2, p. 246-255, mars 2011, doi: 10.2514/1.49490.

[3] Van Eesbeek M. and Zwaal A., "Outgassing and contamination model based on residence time," *Proceedings of the 3rd ISMSE*, ESTEC, Noordwick, The Netherlands, 1985, p. 25-34.

[4] Tondu T., Vanhove E., Roussel J. F., and Faye D., "Mixture Effects in Contaminant Reemission," *J Spacecr Rockets*, vol. 53, nº 6, p. 1172-1177, nov. 2016, doi: 10.2514/1.A33507.

[5] Vanhove E., Tondu T., Roussel J. F., Faye D., and Guigue P., "In Situ Real-Time Quantitative and Qualitative Monitoring of Molecular Contamination," *J Spacecr Rockets*, vol. 53, nº 6, p. 1166-1171, nov. 2016, doi: 10.2514/1.A33505.

[6] Vanhove E., Grosjean E., Rioland G., and Faye D., "Comparison of molecular contamination models based on TGA/MS experiments," *Proceedings of the 14th ISMSE*, Biarritz, France, oct. 2018, p. 9.

[7] Garrett J. W., A. Glassford P. M., and Steakley J. M., "ASTM-E-1559 Method for Measuring Material Outgassing/Deposition Kinetics," *J. IEST*, vol. 38, nº 1, p. 19-28, 1995.

[8] Loerting T. and Giovambattista N., "Amorphous ices: experiments and numerical simulations," *J. Phys.: Condens. Matter*, vol. 18, nº 50, p. R919-R977, déc. 2006, doi: 10.1088/0953-8984/18/50/R01.

[9] NIST Mass Spectrometry Data Center and Wallace W. E., "Octane," in *NIST Chemistry WebBook*, Eds. Linston P.J. and Mallard W.G.., vol. 69, Gaithersburg MD, 20899: National Institute of Standards and Technology. Accessed on April 7th 2022. [Online]. Available at: https://webbook.nist.gov/cgi/cbook.cgi?ID=C111659&Units=SI&Mask=200#Mass-Spec

[10] NIST Mass Spectrometry Data Center and Wallace W. E., "Methanamine, N-hydroxy-N-methyl-" in *NIST Chemistry WebBook*, Eds. Linston P.J. and Mallard W.G.., vol. 69, Gaithersburg MD, 20899: National Institute of Standards and Technology. Accessed on April 7th 2022. [Online]. Available at:. https://webbook.nist.gov/cgi/cbook.cgi?ID=C5725962&Mask=200#Mass-Spec

[11] NIST Mass Spectrometry Data Center and Wallace W. E., "Acetone" in *NIST Chemistry WebBook*, Eds. Linston P.J. and Mallard W.G.., vol. 69, Gaithersburg MD, 20899: National Institute of Standards and Technology. Accessed on April 7th 2022. [Online]. Available at: https://webbook.nist.gov/cgi/cbook.cgi?ID=C67641&Units=SI&Mask=200#Mass-Spec

[12] NIST Mass Spectrometry Data Center and Wallace W. E., "Propanal". in *NIST Chemistry WebBook*, Eds. Linston P.J. and Mallard W.G.., vol. 69, Gaithersburg MD, 20899: National Institute of Standards and Technology. Accessed on April 7th 2022. [Online]. Available at: https://webbook.nist.gov/cgi/cbook.cgi?ID=C123386&Mask=200#Mass-Spec